ARKIV FÖR FYSIK Band 17 nr 2

Communicated 2 December 1959 by ERIK RUDBERG and KAI SIEGBAHN

Atomic level energies in rare earth elements

By PÄR BERGVALL and STIG HAGSTRÖM

With 9 figures in the text

ABSTRACT

The L_I, L_{II} and L_{III} level energies have been measured in the oxides of stable rare earth elements ($57 \leqslant Z \leqslant 60$, $62 \leqslant Z \leqslant 71$), employing the photo electron method. The L_{II}–L_{III} energy differences are found to agree within 0.5 eV with the $K\alpha_1 - \alpha_2$ X-ray emission energy differences. A comparison with theoretical predictions is also made, and the possibility of a quantitative estimate of nuclear size effects on the fine structure is discussed. The L levels and the K level (obtained by addition of the $K\alpha$ lines) are compared with data from X-ray absorption spectroscopy, showing systematic discrepancies especially for the L_I level.

1. Introduction

The study of atomic binding energies by means of the photo electron method has been developed to a high precision by Siegbahn, Nordling, and Sokolowski [1–6]. Measurements have been performed on K and L levels of 4th, 5th, and 6th period elements, and on L, M, and N levels in uranium. Both metals and oxides have been studied, and chemical effects have been established on the level energies. The present investigation is an extension of the previous systematic studies to the rare earth elements. Determinations of all three L levels have been made, and by addition of the L_{III} and L_{II} level energies to the $K\alpha_1$ and α_2 X-ray transition energies recently measured by Bergvall [7], the K levels are obtained. Because of the reactivity of the metals to air it has not been possible to use the pure elements, and the investigation is therefore confined to the metal oxides.

2. Experimental procedure

For a description of the apparatus and experimental procedure the reader is referred to the previous reports [3, 5]. Here only a few pertinent details shall be discussed.

2.1. *Choice of anode in the X-ray tube*

The anode in the X-ray tube must fulfill several conditions. The energy of the emitted characteristic radiation should exceed the electron binding energy to be measured by at least 3.5 keV, the low energy limit set for detection by the GM counter window. With increasing electron energies, however, the widths of the photo electron lines increase, and the contribution of the natural line width of the X-ray line is enlarged if we choose an anode of high atomic number. The range of suitable elements is thus very limited. Furthermore, the anode material must be able to stand a load of about 1.5 kW, being a good heat conductor and showing no chemical or mechanical changes for hours of operation.

The L level energies of the rare earths range from 5.5 keV to 10.9 keV. The lightest element which is suitable as an anode and with sufficient $K\alpha_1$ line energy is zirconium. The molybdenum $K\alpha_1$ line has an energy of 17.5 keV which, it is true, exceeds the zirconium line by 1.7 keV, but has the great advantage of being regarded as a standard reference line with a well-established wavelength value. This line is therefore the most suitable for the study of the higher energy levels. For the levels of lower energy, however, it would be desirable to use softer radiation. We consider first $K\alpha_1$ line emission and look for a suitable anode of an atomic number lower than 40. The only possible element is germanium, but, unfortunately, the only rare earth in which we can reach all three L levels employing Ge $K\alpha_1$ radiation is the lightest: lanthanum. A $K\beta_1$ line can not be used because of the close proximity of the β_3.

The possibility of using the $L\alpha_1$ line of a heavy element was therefore investigated. A recording of the Ce L_{III} level was made, using the Mo $K\alpha_1$ and Bi $L\alpha_1$ lines respectively. The results are depicted in Fig. 3*c* and Fig. 3*d*. In view of the low melting point of bismuth metal, the anode current had to be kept at half the value used for molybdenum, compensated by double the counting time. The width of the Bi photo electron line is seen to be only two thirds of that of the Mo line. Nevertheless it is apparent from the low intensity and signal to background ratio that the Bi $L\alpha_1$ line represents no advantage over the Mo $K\alpha_1$ line which was therefore used throughout the investigation.

2.2. *Use of filters*

In order to reduce the background of photo electrons ejected by the high energy continuous bremsstrahlung and to some extent by the $K\beta$ lines, a filter should be inserted between the anode and the converter. It should have its K absorption discontinuity slightly higher than the Mo $K\alpha_1$ energy. In Fig. 1 are shown two recordings of the Yb L_{III} photo line with and without use of a zirconium filter, 0.06 mm thick. The signal is reduced, but the signal to background ratio is increased with a factor of 2 in favour of the filter. The same counting time is used in both recordings, and as a measure of the quality of the profiles the signal (excluding background) to the statistical error at the peak can be used. The gain in this ratio is only 10 % in favour of the filter employed. A window of sufficient thickness has to be used to keep down the background of electrons which causes an excessive counting rate of the GM counter. A zirconium window of 0.03 mm thickness was used for this purpose.

2.3. *Source preparation and identification*

The rare earth metals were supplied by Johnson, Matthey & Co., Ltd, London, and Research Chemicals Inc. division of the Nuclear Corporation of America, Inc., Burbank, California, USA, in the highest degree of purity available.

The converters were prepared by evaporation in vacuum of metal filings on to a 20 μ aluminium strip. The thicknesses obtained were estimated to be of the order of 100–200 Ångström units. After a brief exposure to air, the converters were inserted

Table 1. Sample identification by electron diffraction. Spacings (d) and intensities (I), compare diagram 2.

Present	A.S.T.M.X-ray Powder Data File				
Sample	CeO_2			Ce	
d, Å.U.	d, Å.U.	I	hkl	d, Å.U.	I
3.12	3.12	100	111	3.20	100
2.71	2.71	29	200	2.96	16
1.91	1.91	51	220	2.81	72
1.63	1.63	44	311	2.47	16
1.57	1.56	5	222	2.25	16
1.36	1.35	5	400	1.96	24
1.24	1.24	15	331	1.85	40
1.21	1.21	6	420	1.68	16
1.11	1.10	12	422	1.57	8
1.05	1.04	9	511		
0.96	0.96	5	440		
0.92	0.92	13	531		
0.86	0.86	7	620		

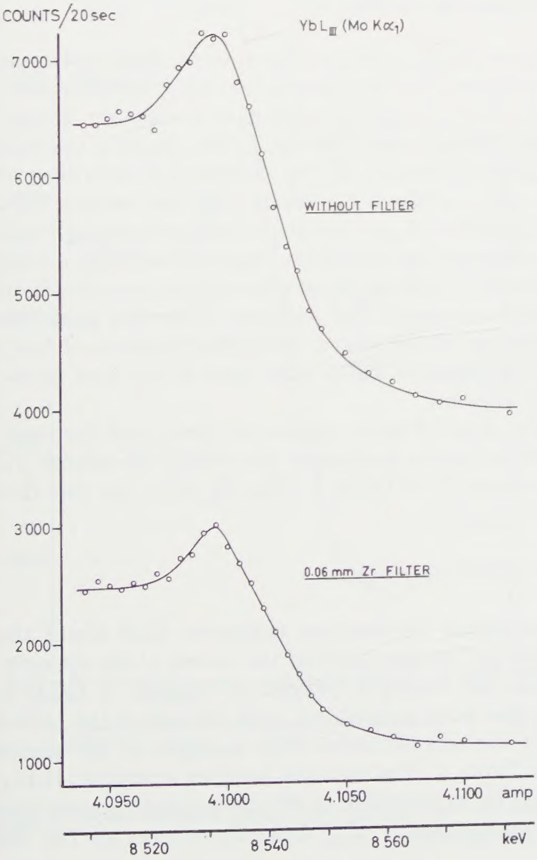

Fig. 1.

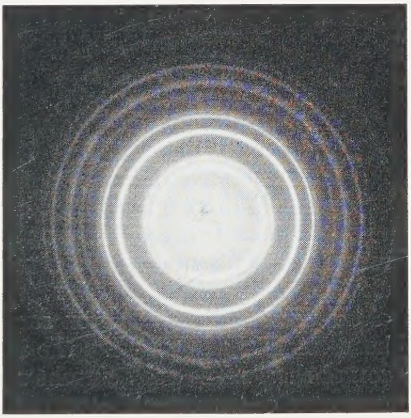

Fig. 2 a.

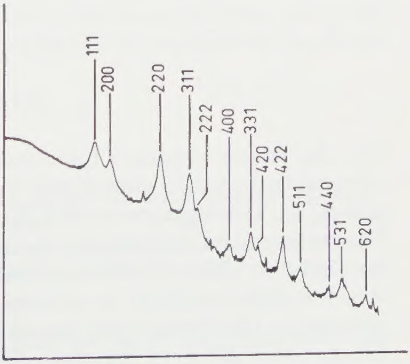

Fig. 2 b.

Fig. 1. Yb L_{III} (Mo $K\alpha_1$) with and without a 0.06 mm thick zirconium filter.

Fig. 2. (a) Electron diffraction pattern from a sample obtained by evaporation of cerium. (b) Photometric recording of the pattern in (a).

in the spectrometer tank. The temperature of the converter mounting during a measurement was determined, with the aid of a thermocouple, to be about 80°C.

For the chemical identification the A.S.T.M. X-ray powder data file [8] and information generously provided by Lindsay Chemical Division, USA [9], were used. A sample, evaporated on formvar and handled under the same conditions as the converter, was subjected to electron diffraction. In no case could traces of metal lines be detected in the diffraction patterns, and all of the reflexions obtained, at least four in each pattern, were identified as belonging to one and the same compound. The reproducibility of the photo electron line energies with time and with different sources shows that any temporal changes in the composition of the converter, or differences in the composition of different converters are of negligible influence compared to the statistical uncertainties in the measurements.

One of the diffraction patterns, that for cerium, is reproduced in Fig 2 together with a photometric recording. In Table 1 we find a comparison of the atomic spacings as calculated from this recording, and those listed in the A.S.T.M. file for Ce and CeO_2. The agreement with CeO_2 is complete and the Miller indices have been indicated in Fig. 2*b*. The results of the identifications are found in the first column of Table 2.

3. Experimental results

Four runs on each of the three L level photo electron lines were made using at least two different converters for each element. The line shapes for two of the elements, cerium and lutetium, the first and last of the proper lanthanides, are shown in figs. 3 and 4. The L_{III} line is the most intense in both cases, but the L_I line shows a marked increase in relative intensity for the lighter element. In Fig. 5 is seen a recording of the Pr L_{III}(Mo $K\alpha_1$) line including the Pr L_{III}(Mo $K\alpha_2$) line on the low energy side. The first discrete energy loss line is well resolved from the photo line even though this recording represents one of the most unfavourable instances, namely one with a high electron energy. In view of the discussion by Nordling [5] on this subject, no correction of the peak position has been considered necessary. The position of the line peak has been established by taking the intersection of the curve with the diameter of horizontal chords. The peak current values are listed in Table 2 for each of the four measurements of the three L levels in each element.

As a calibration line the $KL_{II}L_{III}(^1D_2)$ Auger line in copper has been used throughout the investigation, employing the triple source technique previously described [2]. The peak current values are given in column 6 of Table 2. The $B\varrho$ value for this line has been determined by Nordling [5]:

$$283.803 \pm 0.010 \text{ gauss-cm}$$

The $B\varrho$ values obtained have been corrected for residual magnetic field along the electron trajectories when external fields are compensated at the center of the spectrometer [3]. The mean corrected $B\varrho$ values are found in the second column of Table 3. Conversion from momentum to energy has been carried out with the aid of the tables by Gerholm [10] with interpolation to the second order. The energies of the photo electron lines are given in column 3 of Table 3. The electron binding energies (B.E.), referred to the Fermi level, are obtained by subtraction of the photo electron energies (E_{photo}) and the work function of the spectrometer (ϕ_{sp}) from the energy of the Mo

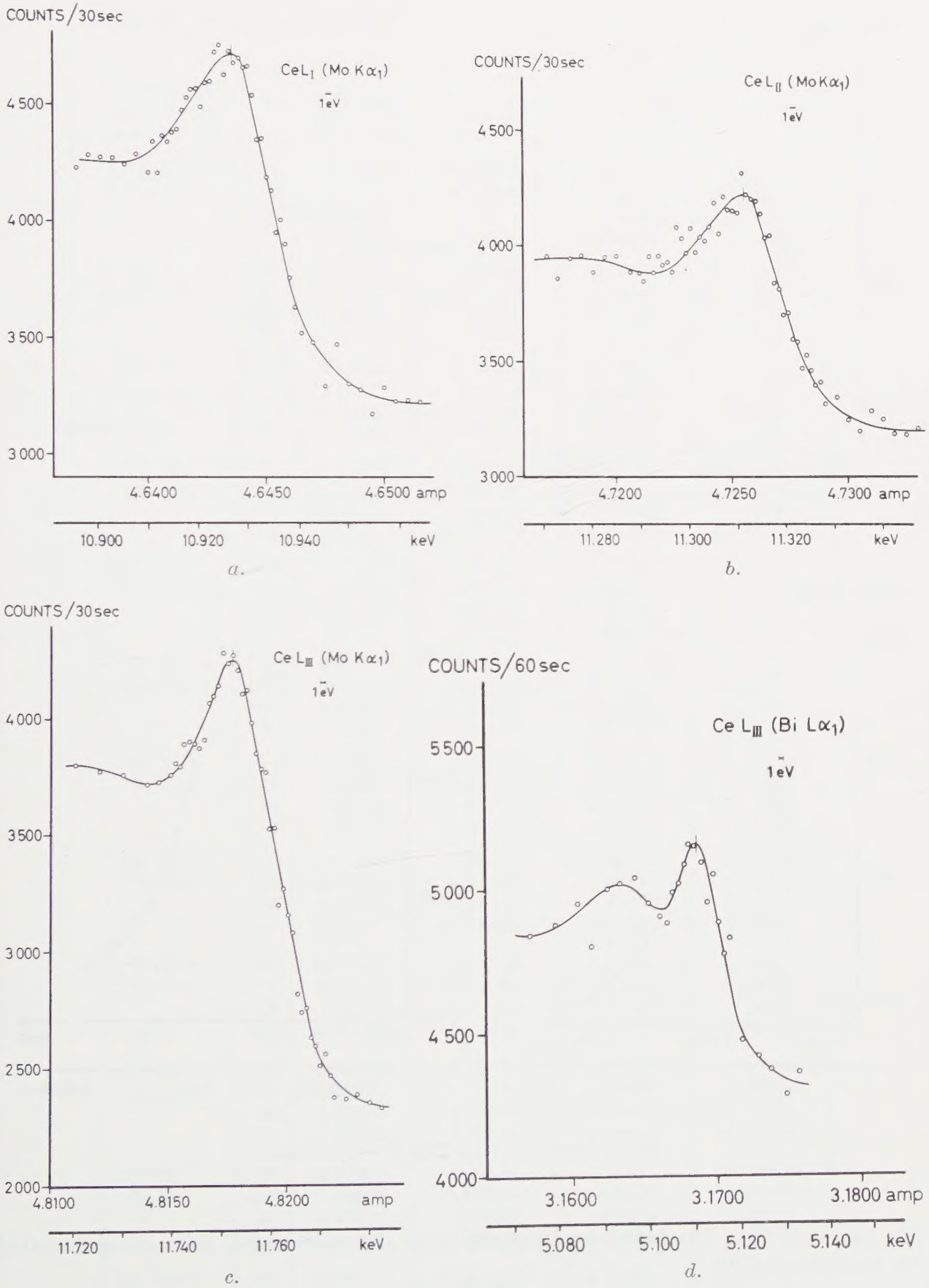

a. *b.* *c.* *d.*

Fig. 3. Photo electron lines from cerium, (*a*), (*b*), and (*c*) with the use of Mo$K\alpha_1$ radiation and (*d*) with Bi $L\alpha_1$.

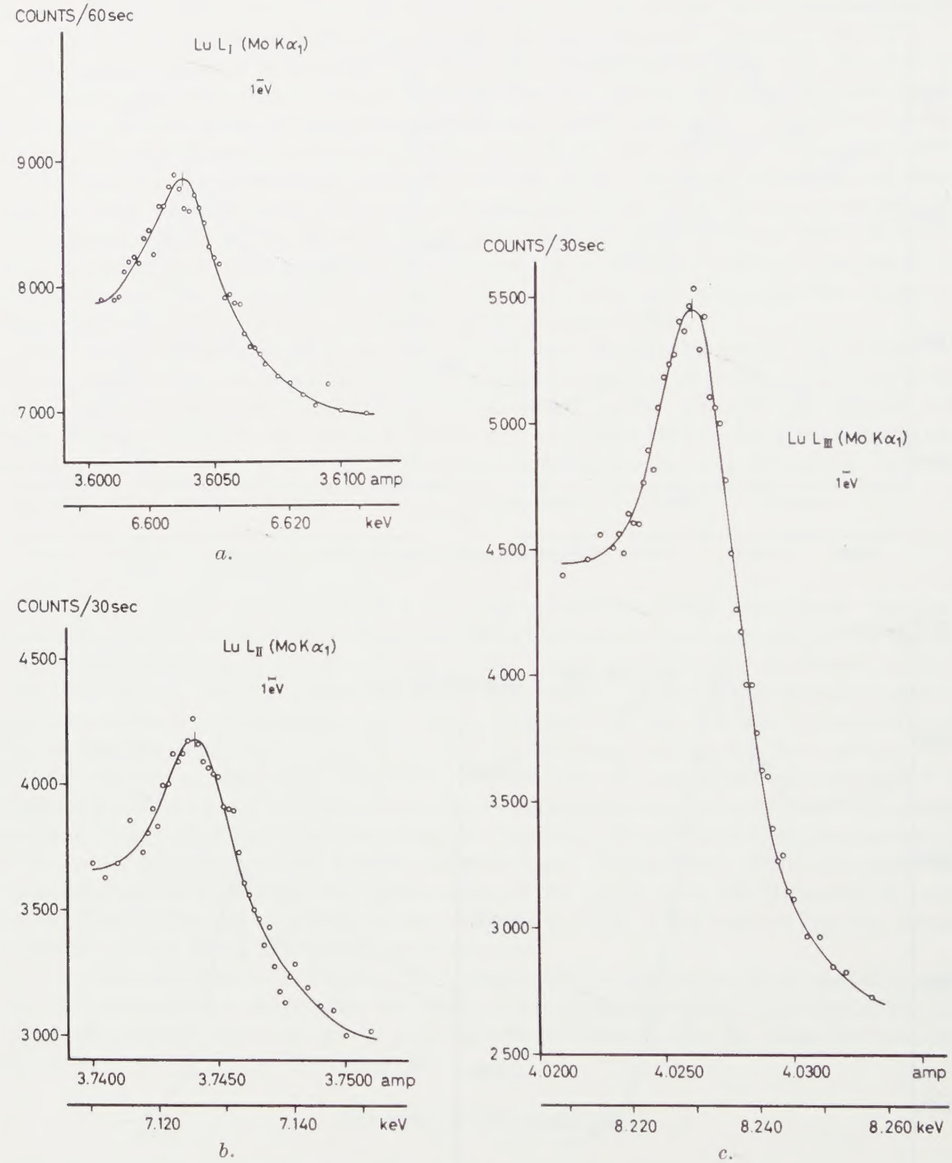

Fig. 4. Photo electron lines from lutetium.

$K\alpha_1$ emission line. The latter is calculated from the wavelength value recommended by Sandström [11]:

707.831 XU

17.4970 keV

Table 2. Peak current values of photo electron and calibration lines.

Element (Compound)	♯	I_{L_I} (amp)	$I_{L_{II}}$ (amp)	$I_{L_{III}}$ (amp)	I_{cal} (amp)
57 La	174	4.70365	4.78280	4.86710	3.71880
(La_2O_3)	174	4.70355	4.78270	4.86698	3.71877
	175	4.70413	4.78318	4.86783	3.71956
	175	4.70436	4.78320	4.86772	3.71948
58 Ce	172	4.64358	4.72550	4.81762	3.71887
(CeO_2)	172	4.64613	4.72792	4.82040	3.72106
	173	4.64348	4.72552	4.81756	3.71916
	173	4.64365	4.72530	4.81754	3.71922
59 Pr	169	4.58080	4.66600	4.76655	3.71848
(Pr_6O_{11})	170	4.58132	4.66642	4.76710	3.71864
	170	4.58123	4.66628	4.76700	3.71855
	171	4.58133	4.66628	4.76710	3.71895
60 Nd	167	4.51760	4.60588	4.71558	3.71864
(Nd_2O_3)	167	4.51723	4.60551	4.71572	3.71850
	176	4.51761	4.60573	4.71578	3.71884
	176	4.51754	4.60590	4.71563	3.71878
62 Sm	159	4.38414	4.47953	4.61002	3.72102
(Sm_2O_3)	159	4.38340	4.47880	4.60950	3.72058
	160	4.38434	4.47958	4.61030	3.72180
	160	4.38437	4.47990	4.61055	3.72192
63 Eu	161	4.31035	4.40932	4.55187	3.71991
(Eu_2O_3)	161	4.31033	4.40933	4.55190	3.72005
	165	4.30866	4.40780	4.55030	3.71882
	165	4.30880	4.40809	4.55031	3.71875
64 Gd	138	4.23300	4.33600	4.49125	3.71815
(Gd_2O_3)	138	4.23282	4.33615	4.49100	3.71815
	139	4.23420	4.33765	4.49265	3.71955
	139	4.23438	4.33751	4.49254	3.71958
65 Tb	150	4.15747	4.26498	4.43397	3.72099
(Tb_2O_3)	150	4.15725	4.26509	4.43373	3.72085
	151	4.15633	4.26382	4.43257	3.72013
	151	4.15618	4.26388	4.43281	3.72015
66 Dy	152	4.07500	4.18704	4.37100	3.72048
(Dy_2O_3)	152	4.07499	4.18712	4.37099	3.72048
	153	4.07543	4.18747	4.37128	3.72089
	153	4.07533	4.18753	4.37141	3.72094
67 Ho	154	3.99065	4.10748	4.30785	3.72178
(Ho_2O_3)	154	3.99072	4.10750	4.30806	3.72178
	155	3.98964	4.10645	4.30672	3.72068
	155	3.98930	4.10616	4.30656	3.72059
68 Er	157	3.90226	4.02450	4.24280	3.72301
(Er_2O_3)	157	3.90213	4.02424	4.24250	3.72315
	158	3.90082	4.02285	4.24111	3.72185
	158	3.89961	4.02193	4.23990	3.72071
69 Tm	148	3.80719	3.93506	4.17268	3.72174
(Tm_2O_3)	149	3.80545	3.93292	4.17062	3.72017
	149	3.80540	3.93325	4.17066	3.72029
	149	3.80537	3.93321	4.17073	3.72023

(Table 2, cont.)

Element (Compound)	♯	I_{L_I} (amp)	I_{L_II} (amp)	I_{L_III} (amp)	I_{cal} (amp)
70 Yb	140	3.70476	3.83882	4.09742	3.71769
(Yb_2O_3)	140	3.70532	3.83867	4.09740	3.71772
	141	3.70786	3.84145	4.10011	3.72072
	141	3.70717	3.84082	4.09953	3.72002
71 Lu	146	3.60370	3.74405	4.02615	3.72007
(Lu_2O_3)	146	3.60374	3.74405	4.02612	3.72006
	147	3.60649	3.74728	4.02937	3.72309
	147	3.60640	3.74697	4.02932	3.72302

The conversion factor used is the one advocated by DuMond and Cohen 1953 [12]:

$$12372.2\ \mathrm{keV}\cdot\mathrm{XU}$$

The reason for using this value instead of the figure given 1955 by Cohen and DuMond [13] is that within one year we shall probably have an even better value for this conversion factor as a result of the measurements on the λ_g/λ_s ratio being carried out at present by Bearden at Johns Hopkins University, Baltimore, and by Kirkpatrick-DuMond at the California Institute of Technology, Pasadena, USA. All previous photo electron work with the present instrument is based on the 1953 value, and the authors believe that it will lead to less confusion if this figure is used for the time being. Use of the 1955 conversion constant (12372.44 keV·XU) yields higher values for the binding energies, the increase ranging from 0.2 eV (La) to 0.1 eV (Lu) for the L levels, and from 0.8 eV (LA) to 1.1 eV (Lu) for the K levels. The binding energies are given in the 4th and 5th columns of Table 3: energies including the work

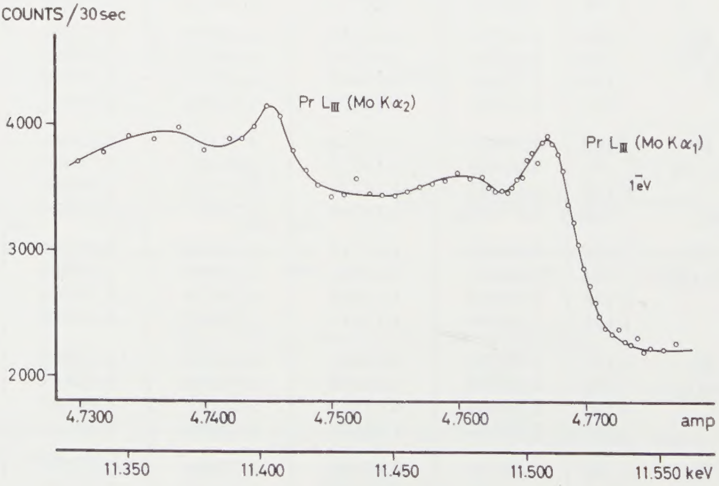

Fig. 5. An extended recording of the Pr L_{III}(Mo $K\alpha_1$) line showing a well resolved characteristic energy loss line and also the photo line from Mo $K\alpha_2$.

Table 3. Mean values of momenta and energies of photo electrons, binding energies.

Level	$B\varrho$ (gauss-cm)	E_{photo} (eV)	B.E. + ϕ_{sp} (eV)	B.E. (eV)	X-ray (eV)
La L_{I}	358.944	11207.8 ± 0.9	6271.2 ± 1.2	**6266.7**	6283.8 (b)
L_{II}	364.975	11583.4 ± 0.9	5895.6 ± 1.2	**5891.1**	5894.6 (b)
L_{III}	371.419	11991.4 ± 0.9	5487.6 ± 1.3	**5483.1**	5489.7 (b)
K			38928.8 ± 1.3	**38924.3**	38933 (d)
Ce L_{I}	354.347	10925.6 ± 0.9	6553.4 ± 1.1	**6548.9**	6561.4 (b)
L_{II}	360.591	11309.8 ± 0.9	6169.2 ± 1.2	**6164.7**	6165.4 (b)
L_{III}	367.628	11750.5 ± 0.9	5728.5 ± 1.2	**5724.0**	5728.7 (b)
K			40447.6 ± 1.3	**40443.1**	40452 (d)
Pr L_{I}	349.624	10639.2 ± 0.8	6839.8 ± 1.1	**6835.3**	6846.4 (c)
L_{II}	356.117	11033.9 ± 0.9	6445.1 ± 1.2	**6440.6**	6443.5 (c)
L_{III}	363.801	11509.8 ± 0.9	5969.2 ± 1.2	**5964.7**	5968.8 (c)
K			41994.8 ± 1.3	**41990.3**	42001 (d)
Nd L_{I}	344.761	10348.3 ± 0.8	7130.7 ± 1.1	**7126.2**	7144.5 (c)
L_{II}	351.497	10752.3 ± 0.9	6726.7 ± 1.1	**6722.2**	6727.3 (c)
L_{III}	359.885	11266.1 ± 0.9	6212.9 ± 1.2	**6208.4**	6215.0 (c)
K			43573.2 ± 1.3	**43568.7**	43573 (d)
Sm L_{I}	334.342	9738.0 ± 0.8	7741.0 ± 1.0	**7736.5**	7754.9 (c)
L_{II}	341.617	10162.2 ± 0.8	7316.8 ± 1.1	**7312.3**	7281.6 (c)
L_{III}	351.578	10757.3 ± 0.9	6721.7 ± 1.1	**6717.2**	6721.1 (c)
K			46838.9 ± 1.2	**46834.4**	46848 (d)
Eu L_{I}	328.831	9422.5 ± 0.7	8056.5 ± 1.0	**8052.0**	8060.6 (g)
L_{II}	336.392	9856.6 ± 0.8	7622.4 ± 1.0	**7617.9**	7619.8 (g)
L_{III}	347.261	10497.4 ± 0.8	6981.6 ± 1.1	**6977.1**	6980.5 (g)
K			48523.2 ± 1.2	**48518.7**	48518 (f)
Gd L_{I}	323.082	9098.8 ± 0.7	8380.2 ± 1.0	**8375.7**	8386.2 (g)
L_{II}	330.959	9543.7 ± 0.8	7935.3 ± 1.1	**7930.8**	7930.9 (g)
L_{III}	342.791	10231.4 ± 0.8	7247.6 ± 1.1	**7243.1**	7242.8 (g)
K			50243.3 ± 1.2	**50238.8**	50232 (f)
Tb L_{I}	317.081	8766.7 ± 0.7	8712.3 ± 0.9	**8707.8**	8716.5 (g)
L_{II}	325.290	9222.4 ± 0.7	8256.6 ± 1.0	**8252.1**	8252.5 (g)
L_{III}	338.167	9960.0 ± 0.8	7519.0 ± 1.0	**7514.5**	7515.2 (g)
K			51999.9 ± 1.2	**51995.4**	52002 (f)
Dy L_{I}	310.840	8427.8 ± 0.7	9051.2 ± 0.9	**9046.7**	9065.2 (b)
L_{II}	319.390	8893.8 ± 0.7	8585.2 ± 0.9	**8580.7**	8583.5 (b)
L_{III}	333.415	9684.6 ± 0.8	7794.4 ± 1.0	**7789.9**	7796.0 (b)
K			53792.1 ± 1.2	**53786.6**	53792 (f)
Ho L_{I}	304.307	8080.0 ± 0.6	9399.0 ± 0.8	**9394.5**	9399.2 (g)
L_{II}	313.216	8556.1 ± 0.7	8922.9 ± 0.9	**8918.4**	8916.3 (g)
L_{III}	328.499	9403.6 ± 0.7	8075.4 ± 1.0	**8070.9**	8067.4 (g)
K			55621.5 ± 1.2	**55617.0**	55618 (f)
Er L_{I}	297.452	7722.8 ± 0.6	9756.2 ± 0.8	**9751.7**	9756.1 (g)
L_{II}	306.766	8210.0 ± 0.6	9269.0 ± 0.9	**9264.5**	9262.0 (g)
L_{III}	323.402	9116.6 ± 0.7	8362.4 ± 1.0	**8357.9**	8357.3 (g)
K			57489.2 ± 1.2	**57484.7**	57486 (f)
Tm L_{I}	290.306	7358.7 ± 0.6	10120.3 ± 0.8	**10115.8**	10120.4 (g)
L_{II}	300.050	7857.2 ± 0.6	9621.8 ± 0.8	**9617.3**	9616.9 (g)
L_{III}	318.169	8826.4 ± 0.7	8652.6 ± 0.9	**8648.1**	8649.5 (g)
K			59393.4 ± 1.2	**59388.9**	59339 (a)

(Table 3, cont.)

Level	$B\varrho$ (gauss-cm)	E_{photo} (eV)	B.E. + ϕ_{sp} (eV)	B.E. (eV)	X-ray (eV)
Yb L_{I}	282.829	6987.1 ± 0.6	10491.9 ± 0.7	**10487.4**	10490.2 (e)
L_{II}	293.029	7496.4 ± 0.6	9982.6 ± 0.8	**9978.1**	9976.0 (e)
L_{III}	312.767	8531.7 ± 0.7	8947.3 ± 0.9	**8942.8**	8944.0 (e)
K			61335.5 ± 1.2	**61331.0**	61303 (f)
Lu L_{I}	274.921	6604.3 ± 0.5	10874.7 ± 0.7	**10870.2**	10873.8 (e)
L_{II}	285.635	7125.4 ± 0.6	10353.6 ± 0.7	**10349.1**	10344.6 (e)
L_{III}	307.150	8230.5 ± 0.7	9248.5 ± 0.9	**9244.0**	9242.0 (e)
K			63317.5 ± 1.2	**63313.0**	63304 (f)

(a) Cabrera (1923) oxide, [14].
(b) Coster *et al.* (1923) salts, [15].
(c) Nishina (1925) sulphates, [16].
(d) Rouault (1939) oxalates, carbonate [17].
(e) Allais (1941) [18].
(f) Manescu (1943–1944) oxides, [19].
(g) Sakellaridis (1953–1954) oxides, [20].

function of the spectrometer (B.E. + ϕ_{sp}) in column 4, and energies referred to the Fermi level (B.E.) in column 5. The K levels which are included are obtained from the mean of the $K\alpha_2 + L_{\text{II}}$ and $K\alpha_1 + L_{\text{III}}$ energies. The K emission line energies have been computed from the wavelength values given by Bergvall [7], here also using the 1953 conversion constant.

4. Error estimate

As a consequence of the constant resolving power of the spectrometer, the photo electron line widths increase linearly with electron momentum. To some extent this effect is reduced by the decrease of natural level widths with decreasing atomic number. The increasing line widths correspond to an increasing absolute uncertainty in the localization of line peaks for the high electron energies corresponding to low binding energies. This uncertainty is revealed in the scatter of the experimental values of photo electron momenta around the mean values. The relative spread in momentum, which is constant, has been calculated for the whole of the experimental material and corresponds to a standard deviation of $4 \cdot 10^{-5}$. A χ^2 test of the distribution, compared with a Gaussian curve of the same standard deviation, yields significance at the 40 % level, in support of a purely statistical nature of the dispersion.

The standard deviation of the mean of four measurements is accordingly $2 \cdot 10^{-5}$ and as the error of the mean is assigned to be $4 \cdot 10^{-5}$, corresponding to a confidence coefficient of 93 %. The corresponding absolute energy errors are given in the third column of Table 3. The relative error in the calibration constant, given by Nordling, is $3.5 \cdot 10^{-5}$, and this is included quadratically in the errors cited for the binding energies in the fourth column of the same table. Uncertainties in the fundamental constants and X-ray data are disregarded. The K level error limits are obtained by quadratic addition of the K emission line energy uncertainties given by Bergvall [7].

5. An "absolute" check on the calibration

The recording of Ce L_{III}, using Bi $L\alpha_1$ radiation, provides an opportunity for checking the calibration constant and the consistency of the method. Using the wavelength for Bi $L\alpha_1$ given in the Encyclopedia of Physics [11], the following binding energy is obtained:

Ce L_{III}	Bi $L\alpha_1$	Mo $K\alpha_1$ (table 3)
B.E. + ϕ_{sp}:	5727.9 eV	5728.5 eV

The agreement is seen to be well within the error limits.

6. Discussion of results

The rare earth group of elements is unique in the periodic table of natural elements in that the electronic configurations of 14 elements in succession differ only in the state of completion of a (4f) subshell. We should therefore expect a regular variation in the inner atomic level energies from element to element, uninterrupted by the formation of new electronic shells which cause more drastic changes in the screening conditions [21].

The conventional form for the representation of experimental data on atomic energy levels, or "term values", over a range of elements, is the modified Moseley diagram. Based on the assumption that the level energies, or ν/R values, vary essentially as Z^2, an expression of the following form is calculated:

$$\sqrt{E} - aZ - b \tag{1}$$

With the constants a and b suitably adjusted, this should be constant or at least linear with Z, except for discontinuities where new shells start to build up. For K levels of lighter elements and for L_{III} levels, the approximation turns out to be surprisingly good, whereas for L_I and L_{II} levels the presence of higher order terms in Z introduces an increasing curvature in the Moseley lines. Fig. 6 shows modified Moseley diagrams for the K and L level energies of the present work. The constants a and b are differently chosen for each level, but the scale, indicated at the top of the figure, is the same for all the four curves. In order to explain the behaviour of the Moseley lines the higher order terms of Z in the series expansion of the term energies are considered. The Dirac theory yields the following expression as a first approximation for the term binding energies of hydrogenic atoms [22]:

$$E = \frac{\mathrm{Rhc}\,Z^2}{n^2} - \frac{\mathrm{Rhc}\,\alpha^2 Z^4}{n^3}\left(\frac{3}{4n} - \frac{1}{k}\right) \tag{2}$$

$$k = l + 1 \quad \text{for} \quad j = l + 1/2$$
$$k = l \quad \text{for} \quad j = l - 1/2$$

For the case of a many-electron atom the above expression must be modified to take into account the interaction between the electrons. For the present argument it will be sufficient to do so in the classical way due to Sommerfeld, namely by replacing

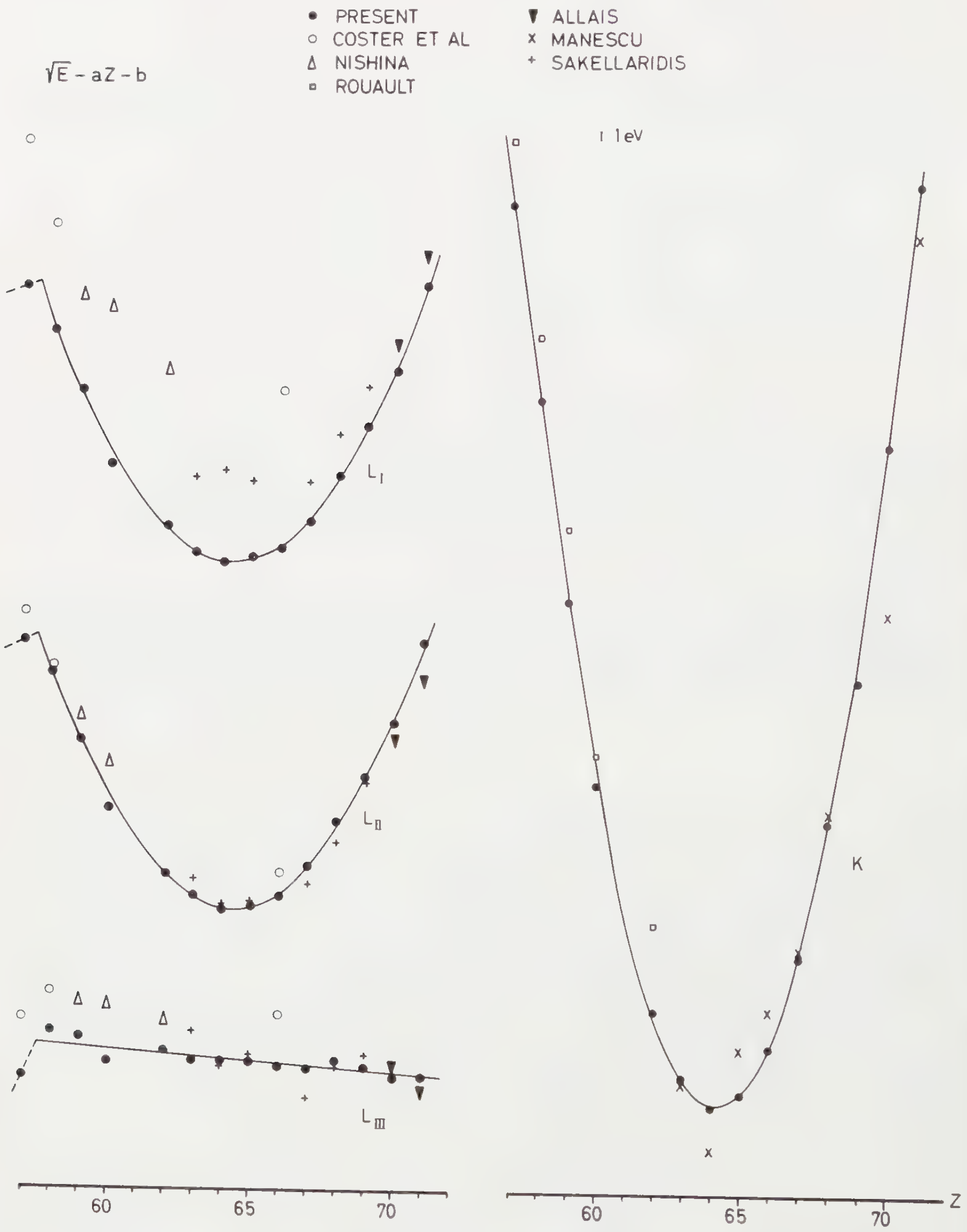

Fig. 6. Modified Moseley diagrams of *K* and *L* levels according to the present measurements and previous X-ray data.

the charge of the nucleus, Z, with an effective charge, $(Z-d)$, where d is a screening number. The term values for the three L levels turn out according to the following:

$$
\begin{aligned}
E_{L_{\mathrm{I}}} &= \frac{\mathrm{Rhc}}{4}\left\{(Z-d_{\mathrm{I}})^2+\frac{5}{64}\,(Z-d'_{\mathrm{I}})^4\,\alpha^2\right\}\\
E_{L_{\mathrm{II}}} &= \frac{\mathrm{Rhc}}{4}\left\{(Z-d_{\mathrm{II}})^2+\frac{5}{64}\,(Z-d'_{\mathrm{II}})^4\,\alpha^2\right\}\\
E_{L_{\mathrm{III}}} &= \frac{\mathrm{Rhc}}{4}\left\{(Z-d_{\mathrm{III}})^2+\frac{1}{64}\,(Z-d'_{\mathrm{III}})^4\,\alpha^2\right\}
\end{aligned}
\qquad (3)
$$

It can be seen immediately from the above expressions that the difference in term values for the L_{I} and L_{II} levels (screening doublets) is entirely due to the different screening of the s and the p orbits. The curvature of the corresponding Moseley lines can be expected to be very similar, a fact demonstrated by Fig. 6. The expressions show that the difference in square roots of term energies for the L_{I} and L_{II} levels should be approximately constant, a relation known as Hertz' law of screening doublets. In fact, a slight linear dependence on Z is obtained, illustrated for the present experimental material in Fig. 7. This dependence on Z is removed if "reduced" term energies (that is, reduced by the appropriate relativity corrections) are used [21].

Considering next the term energy expressions, eq. (3) for the L_{III} level, it is seen that the coefficient for the α^2Z^4 term is only one fifth compared with that of the L_{I} and L_{II} levels. The coefficients for the next terms in the series expansion, in α^4Z^6, differ by a factor of 21. This explains the difference in curvature of the Moseley lines for the L_{I} L_{II} levels and the L_{III} level, although it does not explain why a straight line is obtained in the latter case, as seen in Fig. 6.

The fact that the L_{II} and $\mathrm{L}_{\mathrm{III}}$ orbits are both $2p$, differing only in quantum number j, indicates that the screening terms d_{II} and d_{III} are the same for both levels and that a relatively simple expression for the level separation will result as the main energy terms cancel each other. For a calculation of the level separation (spin doublet splitting), however, eq. (3) is not sufficiently accurate, and the exact formula given by Sommerfeld has therefore been used:

$$
\Delta E=\frac{\mathrm{Rhc}}{\alpha^2}\left\{\sqrt{4-\alpha^2\,(Z-d)^2}-[2+2\sqrt{1-\alpha^2\,(Z-d)^2}]^{1/2}\right\} \qquad (4)
$$

For hydrogenic atoms $(d=0)$, this expression is identical with the result obtained by the Dirac theory [22]. Sommerfeld has shown [23] that a comparison with experimental data gives an almost constant value for the screening term d for all of the heavier elements of the periodic table. It seems reasonable to expect a constant screening for the rare earths in particular. The third column of Table 4 gives values for ΔE according to eq. (4), the screening number d being adjusted to give the closest agreement with the experimental results. This value is 3.58. The difference is well within experimental errors or 0.05 %, a remarkable agreement considering the rather crude model used to account for the screening. It should be noted that a series expansion of eq. (4), containing even four terms of increasing powers of $(Z-d)$, does not give this overall agreement for a constant value of d. A graphical representation is found in Fig. 8, where the circles represent experimental data and the solid line the Sommerfeld theory.

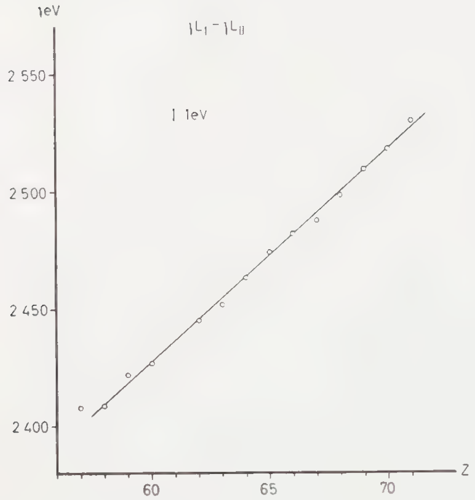

Fig. 7. Diagram illustrating Hertz' law of screening doublets.

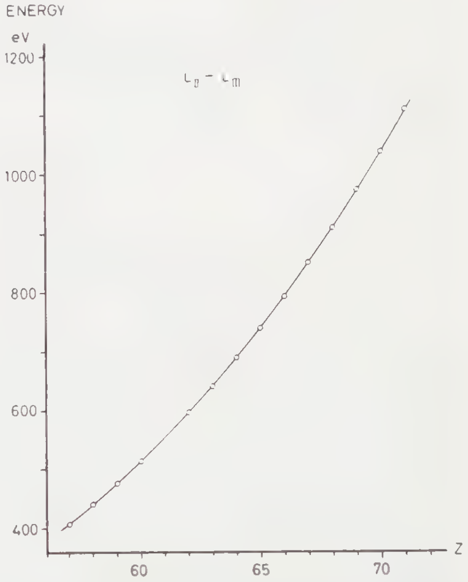

Fig. 8. Experimental values of the energy difference between the L_{II} and L_{III} levels as a function of Z. The solid line represents the Sommerfeld theory according to eq. (4).

In this classical treatise "Atombau und Spektrallinien" [23], Sommerfeld goes a step further in the calculations by computing, from experimental data, values of the screening numbers in the main energy term of eq. (3). The screening varies with Z in a monotonous but non-linear manner. To overcome this variation, a separation into

Table 4. $L_{II} - L_{III}$ level energy difference in eV as obtained by the present method, by K X-ray spectroscopy and by Sommerfeld theory.

Z		Present L_{II} L_{III}	Bergvall [7] $K\alpha_1 - \alpha_2$	Sommerfeld $d - 3.58$
57	La	408.0	407.6	407.7
58	Ce	440.7	441.0	440.9
59	Pr	475.9	476.4	476.2
60	Nd	513.7	513.8	513.6
62	Sm	595.1	595.6	595.6
63	Eu	640.8	640.3	640.5
64	Gd	687.7	687.4	687.7
65	Tb	737.6	737.4	737.9
66	Dy	790.8	790.7	790.9
67	Ho	847.5	847.1	847.0
68	Er	906.6	906.6	906.2
69	Tm	969.2	969.1	968.9
70	Yb	1035.3	1035.0	1034.9
71	Lu	1105.1	1104.7	1104.6

outer and inner screening is discussed by Pauling and Goudsmit [21]. Knowledge of mean radii of the outer electronic orbits is required for an estimate of the outer screening. The separation yields screening numbers for the inner shells, which are due to internal screening only, and which are constant with Z as required by our model.

According to Condon and Shortley [24], it must be considered futile to carry the calculations of screening terms further and try to obtain theoretical expressions to fit the experimental level energies. Nevertheless, screening parameters in hydrogenic wave functions have proved useful for obtaining approximations, sometimes being very good as they stand [25], but often serving as a starting point for further calculations [26, 27].

A different approach to the problem of extending the Sommerfeld-Dirac expression, eq. (4), to the many-electron atom was made by Christy and Keller [28] in 1942. They used first order perturbation calculations to account for the effect of the interaction between the electrons of the K, L, and M shells on the L_{II} and L_{III} levels. A correction term of the following form is given for the spin doublet splitting, according to eq. (4) with $d = 0$, in Rydberg units.

$$-2\alpha^2 Z^3 f(\alpha Z) + BZ^2 + C\alpha^4 Z^5 \tag{5}$$

The last two terms are included to allow for neglected higher order terms in the interaction Hamiltonian and the effect of outer shell electrons. B is an undetermined constant, while an estimate of C is given. Christy and Keller have tabulated values of the function $f(\alpha Z)$ for a number of Z values. To find this function for the present atomic numbers, an interpolation procedure given by Shacklett and DuMond [29, 30] has been followed. Correction for the influence of the anomalous moment of the electron has been made to the first order by reducing the experimental data with the Bethe–Longmire expression [31]:

$$\left(1 + \frac{\alpha}{\pi}\right)^{-1} \tag{6}$$

Nuclear size effects on the splitting are, according to the Schawlow-Townes theory [32], only of the order of $3 \cdot 10^{-4}$ for $Z \approx 70$, a negligible amount in the present comparison. To summarize:

$$\left(\frac{\Delta \nu}{R}\right)_{\mathrm{exp}} = \left[\frac{1}{\alpha^2}\left\{\sqrt{4 - \alpha^2 Z^2} - \left(2 + 2\sqrt{1 - \alpha^2 Z^2}\right)^{1/2}\right\} - 2\alpha^2 Z^3 f(\alpha Z) - \right.$$
$$\left. - 0.0356\,\alpha^4 Z^5 + B Z^2\right]\left(1 + \frac{\alpha}{\pi}\right) \tag{7}$$

It was found, however, that an adjustment of the Christy–Keller formula to the present experimental spin doublet splitting energies according to Table 4 was possible only within 0.3 % on the assumption of a constant value of B. Expressed in a different way, a fit to the experimental data gave values of B, varying with Z, according diagram 9.

In the diagram are included X-ray data on the fine structure splitting, for $Z < 57$ according to the Encyclopedia of Physics [11], and for $Z > 71$ according to Shacklett

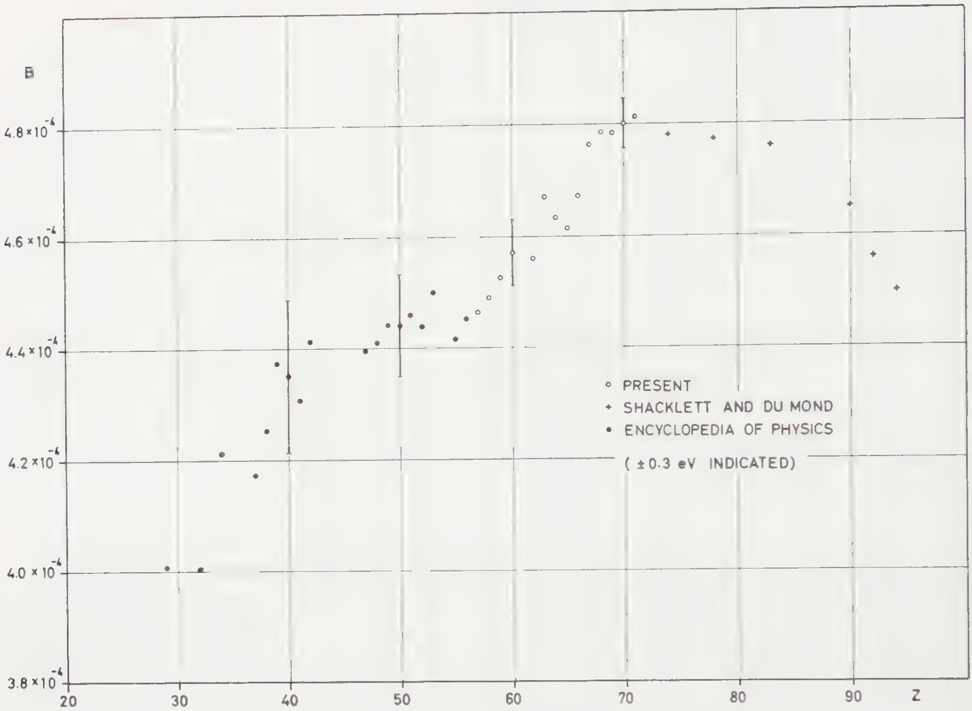

Fig. 9. The value of the parameter B in the Christy-Keller correction to the Sommerfeld expression for the spin doublet splitting. Adjustment has been made to experimental data, present and previous, according to eq. (7). The decrease for high Z-values is caused by nuclear size and quantum electrodynamic effects.

and DuMond [29]. The indicated error limits, ±0.3 eV, are representative, except for the lower values of Z, where the accuracy is sometimes better, and for the measurements by Shacklett and DuMond, who claim an error of the order of 0.1 eV.

The systematic increase in B for $Z < 70$ suggests the presence of neglected higher order terms in the Christy–Keller formula.

The decrease in B for high Z values is explained as nuclear size and quantum electrodynamic effects. The fact that B is not constant, however, tends to make a quantitative estimate of these effects rather uncertain. Shacklett and DuMond [29] made such an estimate under the assumption of a constant B, ($B = 4.7645 \cdot 10^{-4}$). Fig. 9 indicates that the combined nuclear size effects might rather be underestimated by such an assumption. A theoretical calculation of the fine structure splitting for a point nucleus, of sufficient precision to allow for a quantitative separation of the nuclear size effects, is apparently not yet available.

What are probably the most recent theoretical values of atomic binding energies for heavier elements are those obtained by S. Cohen [33] using a relativistic self-consistent calculation of the Hartree type. Unfortunately none of the rare earths is included in the number of atoms investigated. It appears, however, that the agreement with experiment so far is only within 1 % for K and L levels and level differences.

On the basis of the assumption of a regular variation of the term energies with Z, the modified Moseley diagrams serve the purpose of bringing out the scatter of experimental points around a smooth line, drawn according to a "closest fit" as in Fig. 6. Two aspects should, however, be emphasized. First, the present measurements have been carried out on chemical compounds of the elements, involving possible, irregular chemical shifts of the level energies. This may account for some of the spread in the values at the low atomic numbers. Secondly, the subshell $4f$ starts to build up with the element 58 Ce, and we should expect a discontinuity in the diagram between the first and the second element in the row, due to the change in the outer screening conditions. The fact that $4f$ is an *inner* subshell indicates an exceptionally sharp break [21], which can be inferred from diagram 6, and which has been witnessed previously by X-ray spectroscopists.

7. Comparison with X-ray data

Our knowledge of inner atomic level energies, prior to the data from the photo electron method, is based on a combination of X-ray absorption and emission spectroscopy. The absorption discontinuities, such as the K edge for lighter elements or the L_{III} edge for heavier elements have been established with high accuracy, and suitable emission line energies, still more accurately known, have been added or subtracted to obtain the complete term diagrams [11]. It is, however, doubtful whether the atomic states involved in an absorption experiment are identical with the corresponding states in emission. Experimental evidence of discrepancies of this nature as large as several eV has been reported and discussed by Cauchois [34]. There is also the question to consider, into which orbit the electron goes or, in other words, which is the final state of the atom, in an absorption process. Conventionally it has been claimed by X-ray spectroscopists that the inflexion point of lowest energy in an absorption structure should represent the electronic binding energy relative to the Fermi level of the solid [35]. As it has been emphasized by Parratt in a recent review of these problems [36] an atom which takes part in the absorption is to be regarded as an impurity due to the inner electronic vacancy. The final state is consequently one of several discrete *excitation states*, characteristic of the impurity and with nothing in common with the Fermi level of the assembly of undisturbed atoms.

The photo electron method, however, gives by definition [5] the electron binding energies relative to the Fermi level. With this in mind, it is of interest to compare the present measurements with previous X-ray absorption data. The latter are listed in the last column of Table 3, following the review by Sandström in the Encyclopedia of Physics [11]. A graphical representation is found in the modified Moseley diagrams of Fig. 6. It should be noticed that some of the results are obtained from salts, and that a few are rather old, which partly explains the greater scatter of the X-ray data around the Moseley lines. One should also remember that the detailed structure of an absorption edge is still unexplained, and that the interpretation difficulties may sometimes be very great, as for example when the faint L_{I} edge is localized in the middle of the Kronig structure of the L_{II} edge, which happens frequently. The agreement with the present data is surprisingly good, but some systematic deviations are observed, which imply that the two methods do not indeed measure identically the same quantity. It is seen that the X-ray data for the L_{I} level are systematically high, of the order of 5 eV. This indicates the presence of selection rules, which determine the final state of the atom in X-ray absorption, different for an *s* or a *p* electron. Divergent trends in the variation with *Z* are also observed for all of the levels, as the X-ray values seem to lie systematically higher for the lower values of *Z*. Similar systematic discrepancies have also been observed by Nordling [5] and Sokolowski [3].

The atomic states involved in *emission*, are, according to Parratt [36] mostly of the same type, namely corresponding to the removal of an electron to "infinity" in the solid (unexcited or τ states). Parratt suggests that these states are the same as those obtained by the photo electron method. This justifies the procedure in the present work of computing the *K* levels by addition of the emission line energies to the *L* levels according to the photo electron method. Some verification is found in the excellent agreement of the $L_{II} - L_{III}$ level differences with the $K\alpha_1 - \alpha_2$ emission line energy differences, witnessed by Table 4. As the photo electron- and X-ray data are of comparable accuracy, the close agreement gives strong support to both sets of measurements.

ACKNOWLEDGEMENTS

The authors are deeply grateful to Professor Kai Siegbahn for his generous support and encouraging interest in this work. We also wish to thank Dr. Carl Nordling for his experienced help and valuable advice. For skilful assistance with the electron diffraction recordings, it is a pleasure to express our gratitude to Fil. mag. Axel Rönnquist at the Institute of Chemistry of this University.

Institute of Physics, University of Uppsala, Sweden.

REFERENCES

1. Sokolowski, E., Nordling, C., and Siegbahn, K., Arkiv f. Fysik *12*, 301 (1957).
2. Nordling, C., Sokolowski, E., and Siegbahn, K., Arkiv f. Fysik *13*, 483 (1958).
3. Sokolowski, E., Arkiv f. Fysik *15*, 1 (1959).
4. Nordling, C., Arkiv f. Fysik *15*, 241 (1959).
5. Nordling, C., Arkiv f. Fysik *15*, 397 (1959).
6. Nordling, C., and Hagström, S., Arkiv f. Fysik *15*, 431 (1959).
7. Bergvall, P., Arkiv f. Fysik *16*, 57 (1959).
8. A.S.T.M. X-ray Powder Data File, 1st to 8th set, Philadelphia (1958).
9. Lindsay Chemical Division, American Potash & Chemical Corporation, West Chicago, Ill., USA (private communication).
10. Gerholm, T. R., in Beta- and Gamma Ray Spectroscopy, editor K. Siegbahn, North Holland Publ. Co., Amsterdam (1955).
11. Sandström, A. E., in Encyclopedia of Physics, vol. XXX, 78, editor S. Flügge, Springer Verlag, Berlin (1957).
12. DuMond, J. W. M., and Cohen, E. R., Rev. Mod. Phys. *25*, 691 (1953).
13. Cohen, E. R., and DuMond, J. W. M., in Encyclopedia of Physics, vol. XXXV, 1, editor S. Flügge, Springer Verlag, Berlin (1957).
14. Cabrera, J., C. R. *176*, 740 (1923).
15. Coster, D., Nishina, Y., and Werner, S., Z. Physik *18*, 207 (1923).
16. Nishina, Y., Phil. Mag. *49*, 521 (1925).
17. Rouault, M., C.R. *209*, 434 (1939).
18. Allais, M.-L., C.R. *212*, 123 (1941).
19. Manescu, I., C.R. *217*, 69 (1943), *218*, 454 (1944).
20. Sakellaridis, P., C.R. *236*, 1244 (1953), *236*, 1014 (1953), *236*, 1547 (1953), *238*, 2296 (1954).
21. Pauling, L., and Goudsmit, S., "The structure of Line Spectra", McGraw-Hill, New York (1930).
22. Bethe, H. A., and Salpeter, E. E., in Encyclopedia of Physics, vol. XXXV, 88, editor S. Flügge, Springer Verlag, Berlin (1957).

23. SOMMERFELD, A., "Atombau und Spektrallinien", Friedr. Vieweg & Sohn, Braunschweig (1924).
24. CONDON, E. U., and SHORTLEY, G. H., "Theory of Atomic Spectra", Cambridge University Press (1935).
25. ASAAD, W. N., and BURHOP, E. H. S., Proc. Phys. Soc. *71*, 369 (1958).
26. SLATER, J. C., "Quantum theory of Matter", McGraw-Hill, New York (1951).
27. HARTREE, D. R., "The Calculation of Atomic Structures", John Wiley & Sons, New York (1957).
28. CHRISTY, R. F., and KELLER, J. M., Phys. Rev. *61*, 147 (1942).
29. SHACKLETT, R. L., and DUMOND, J. W. M., Phys. Rev. *106*, 501 (1957).
30. SHACKLETT, R. L., Rev. Mod. Phys. *30*, 521 (1958).
31. BETHE, H. A., and LONGMIRE, C., Phys. Rev. *75*, 306 (1949).
32. SCHAWLOW, A. L., and TOWNES, C. H., Phys. Rev. *100*, 1273 (1955).
33. COHEN, S., Bull. Am. Phys. Soc., Ser. II, *2*, 311 (1957), and UCRL report 8389 (1958).
34. CAUCHOIS, Y., Journ. de Phys. *13*, 113 (1952).
35. RICHTMYER, F. K., BARNES, S. W., and RAMBERG, E., Phys. Rev. *46*, 843 (1934).
36. PARRATT, L. G., Rev. Mod. Phys. *31*, 616 (1959).

Tryckt den 25 februari 1960

Uppsala 1960. Almqvist & Wiksells Boktryckeri AB